NIH Public Access
Author Manuscript
Cell Stem Cell. Author manuscript; available in PMC 2015 April 03.

Published in final edited form as:
Cell Stem Cell. 2014 April 3; 14(4): 445–459. doi:10.1016/j.stem.2014.01.007.

Conversion of danger signals into cytokine signals by hematopoietic stem and progenitor cells for regulation of stress-induced hematopoiesis

Jimmy L. Zhao[#1,5], **Chao Ma**[#2], **Ryan M. O'Connell**[4], **Arnav Mehta**[1], **Race DiLoreto**[2], **James R. Heath**[2,3,5], and **David Baltimore**[1,5]

[1]Division of Biology, California Institute of Technology, 1200 E. California Blvd, Pasadena, CA 91125, USA

[2]NanoSystems Biology Cancer Center, California Institute of Technology, 1200 E. California Blvd, Pasadena, CA 91125, USA

[3]Kavli Nanoscience Institute, California Institute of Technology, 1200 E. California Blvd, Pasadena, CA 91125, USA

[4]Department of Pathology, University of Utah, 15 North Medical Drive East, Salt Lake City, UT 84112, USA

[#] These authors contributed equally to this work.

SUMMARY

During an infection, the body increases the output of mature immune cells to fight off the pathogen. Despite convincing evidence that hematopoietic stem and progenitor cells (HSPCs) can sense pathogens directly, how this contributes to hematopoietic cell output remains unknown. Here we have combined mouse models with a single cell proteomics platform to show that in response to toll-like receptor stimulation, short-term HSCs and multipotent progenitor cells produce copious amount of diverse cytokines through the NF-κB signaling. Interestingly, the cytokine production ability of HSPCs trumps mature immune cells in both magnitude and breadth. Among cytokines produced by HSPCs, IL-6 is a particularly important regulator of myeloid differentiation and HSPC proliferation in a paracrine manner and in mediating rapid myeloid cell recovery during neutropenia. This study has uncovered a novel property of HSPCs that enables them to convert danger signals into versatile cytokine signals for regulation of stress hematopoiesis.

© 2014 ll Press. All rights reserved.

[5]Correspondence and request for materials should be addressed to DB baltimo@caltech.edu, JRH heath@caltech.edu, or JLZ jzhao@caltech.edu.

Publisher's Disclaimer: This is a PDF file of an unedited manuscript that has been accepted for publication. As a service to our customers we are providing this early version of the manuscript. The manuscript will undergo copyediting, typesetting, and review of the resulting proof before it is published in its final citable form. Please note that during the production process errors may be discovered which could affect the content, and all legal disclaimers that apply to the journal pertain.

Author Contributions. JLZ, DB, CM, RMO and JRH conceived the study. JLZ, CM and AM designed and performed the experiments. RD helped with data collection. JLZ, DB, CM and JRH analyzed the data. JLZ and DB wrote the manuscript.

NIH-PA Author Manuscript
NIH-PA Author Manuscript
NIH-PA Author Manuscript

NIH-PA Author Manuscript

NIH-PA Author Manuscript

NIH-PA Author Manuscript

INTRODUCTION

Immune cells of the myeloid lineage are often considered the first responders of a host defense against bacterial infection; meanwhile, hematopoietc stem and progenitor cells (HSPCs) may respond in a delayed fashion to ensure sufficient production of myeloid cells consumed during an infection. The response by HSPCs is originally thought to be mainly of a passive response to depletion of downstream immune cells, but more recent evidence suggests that HSPCs may participate directly by sensing systemically elevated cytokines through cytokine receptors and bacterial and viral components through toll-like receptors (TLRs) (King and Goodell, 2011; Nagai et al., 2006).

It is well known that immune cells are potent cytokine producers upon encountering bacteria and viruses. When cytokines produced by immune cells and non-hematopoietic tissues accumulate to sufficient quantity, they circulate back to the bone marrow niche via blood circulation to activate HSPCs. Numerous cytokines, including IL-6, TNF-α, IFN-α, IFN-γ, TGF-β and M-CSF, with the ability to regulate proliferation and differentiation of HSPCs have been identified (Baldridge et al., 2010; Baldridge et al., 2011; Challen et al., 2010; Essers et al., 2009; Maeda et al., 2009; Mossadegh-Keller et al., 2013; Pronk et al., 2011). On the other hand, it is clear now that HSPCs can also respond to TLR stimulation directly, leading to accelerated myeloid cell production *in vitro* (Nagai et al., 2006) and likely *in vivo* as well (Megias et al., 2012). However, it remains unclear how direct pathogen sensing by HSPCs translates into signals directing myeloid differentiation under the stressed conditions. Conventional wisdom would suggest that TLR signaling activates lineage-specific transcriptional factors that can directly regulate differentiation within HSPCs. Currently, little is known about what transcription factors downstream of TLR activation might mediate this process. Alternative, but not mutually exclusive, hypothesis is that TLR stimulation activates a general pro-inflammatory program within HSPCs to induce cytokine production, which can act in an autocrine or paracrine manner to regulate differentiation.

In this study, we have combined extensive mouse genetics and a novel microfluidic single cell proteomics platform to show that HSPCs can directly respond to bacterial components via TLR/NF-κB axis, and in response, HSPCs, specifically ST-HSCs and MPPs, produce copious amount of cytokines. In addition, single cells analysis shows that HSPCs contain heterogeneous subsets based on their different cytokine production profiles. The cytokine production ability of HSPCs is shown to be regulated by NF-κB activity, because p50-deficient HSPCs show significantly attenuated cytokine production while miR-146a-deficient HSPCs display significantly enhanced cytokine production. Interestingly, HSPCs are significantly more potent cytokine producers in both breadth and quantity than the conventional known cytokine producers of the immune system, such as myeloid cells and lymphocytes. Furthermore, we have shown that HSPCs possess TLRs, functional NF-κB signaling and cytokine receptors, an entire cascade of molecules necessary to translate danger signals into cytokine signals. Lastly, we have demonstrated the functional significance of HSPC-produced cytokines, especially IL-6, in promoting myelopoiesis *in vitro* and *in vivo* in neutropenic mice after chemotherapeutic treatment or bone marrow transplant. We believe that this represents a novel mechanism by which HSPCs convert danger signals encountered during an infection into a range of versatile cytokine signals to

NIH-PA Author Manuscript

NIH-PA Author Manuscript

NIH-PA Author Manuscript

ensure efficient stress-induced hematopoiesis. This circumvents both the delay associated with having to wait for systemic cytokine accumulation and the need to "reinvent" the molecular circuitry within HSPCs to convert TLR activation into specific differentiation signals.

RESULTS

Heterogeneity in cytokine production profile among purified HSPCs

To test whether any of the HSPC populations have the capability of cytokine production, we adapted a high-throughput microfluidic-based technology to quantify a panel of up to 15 secreted proteins at the single cell level (Ma et al., 2011). HSPCs are rare cells in bone marrow, with LSK cells (defined as Lineage^{-}Sca1^{+}cKit^{+}), a mixed population of long-term HSCs (LT-HSCs), short-term HSCs (ST-HSCs), multipotent progenitor cells (MPPs) and lymphoid-biased MPPs (LMPPs), accounting for less than 1% and LT-HSCs accounting for less than 0.1% of the total nucleated bone marrow cells. This microfluidic platform allowed us to simultaneously measure a large number of secreted proteins at the single cell level from thousands of phenotypically defined cells. After sorting LSK cells and LT-HSCs (defined as LSK CD150^{+}CD48^{-}) with stringent gating criteria and re-analyzing the sorted fraction for purity (Figure S1A), we loaded the cells onto chips containing several thousand microchambers. After 12 hours of incubation with culture medium containing either lipopolysaccharide (LPS), a TLR-4 ligand, alone or with Pam3CSK4, a TLR-2 ligand, secreted proteins were quantified by an enzyme-linked immunosorbent assay (ELISA)-based method (Ma et al., 2011). At this time, nearly all LSK cells remained undifferentiated by FACS analysis (Figure S2). Interestingly, although very few stimulated LT-HSCs produced cytokines, a significant fraction of LSK cells produced a wide range of cytokines upon TLR stimulation (Figure 1A-C and S3). Cytokine production by LSK cells was stimulation-dependent, because few LSK cells had detectable secretion in the absence of stimulation. Interestingly, while LPS alone was sufficient to stimulate 12.9% of LSK cells to produce cytokines, a combination of LPS and Pam3CSK4 boosted the percentage to 37.9% and many more cells secreted multiple cytokines, suggesting an additive effect of simultaneously stimulating multiple TLRs (Figure 1A-C). Among the 12 cytokines studied, IL-6 was the most prominently induced and was secreted by 21.9% of LPS and Pam3CSK4-stimulated LSK cells, while production of the other cytokines ranged from 7-15% (Figure 1B and 1C).

Among the 12 cytokines in the panel, most are produced by multiple immune cell types. However, some cytokines, such as IL-2, IL-4, IL-17 and IFN-γ are mainly produced by lymphocytes, while IL-1β, IL-6, IL-12, TNF-α and GM-CSF are more abundantly produced by cells of the myeloid lineage (Janeway Jr et al., 2001). Interestingly, when unsupervised clustering analysis was performed on LSK cells, it identified two main cytokine clusters, a cytokine cluster (Group i) including IL-6, TNF-α, IL-12 and GM-CSF, that resembles the production profile of myeloid cells, and a cytokine cluster (Group ii) including IL-2, IL-4, IL-10 and IFN-γ, that resembles the production profile of lymphocytes (Figure 1D). LSK cells were divided into multiple functional subsets differing in their ability to produce Group i and Group ii cytokines, ranging from non-producers (Figure 1D subset 1), Group i producers (Figure 1D subset 2), Group ii producers (Figure 1D subset 3), to super-producers

NIH-PA Author Manuscript

NIH-PA Author Manuscript

NIH-PA Author Manuscript

of all cytokines (Figure 1D, subset 4). When the cells from the four subsets were plotted onto the two-dimensional principal component plane with the two vectors representing the two cytokine groups, subset 2 cells fell into the Group i direction and subset 3 cells fell into the Group ii direction, while subset 4 cells fell in-between the two vector directions (Figure 1D, bottom panels), demonstrating once again the differential cytokine secretion profiles among LSK cells.

LSK cells represent a heterogeneous population comprising LT-HSCs, ST-HSCs, MPPs and LMPPs. They represent cells along a differentiation tree with successive loss of self-renewal ability, while still retaining the full potential to replenish most, if not all, hematopoietic cells (Adolfsson et al., 2005; Forsberg et al., 2006). We next asked whether the LSK heterogeneity based on cytokine production profile correlates with known HSPC subsets. To study this, we separately purified LT-HSCs (LSK $Flt3^{-}CD34^{-}$), ST-HSCs (LSK $Flt3^{-}CD34^{+}$), MPPs (LSK $Flt3^{int}CD34^{+}$) and LMPPs (LSK $Flt3^{hi}CD34^{+}$) from the LSK population and analyzed their cytokine secretion with the single cell microfluidic chips (Figure 2 and S4). We confirmed that LT-HSCs lacked cytokine production using a set of stem cell markers different from those used in Figure 1 because of controversy over what set of markers best defines HSCs. In comparison, ST-HSCs and MPPs were potent cytokine producers while more differentiated LMPPs produced rather modest levels of cytokines (Figure 2A-C and S4). Furthermore, similar to unfractionated LSK cells, ST-HSCs and MPPs remained heterogeneous in terms of cytokine production profile (Figure S4A). These results are succinctly summarized using principal component analysis to reduce the 12-dimentional cytokine intensity dataset from 6 different bone marrow subsets down to 2 principal components (Figure 2D and 2E). Principal component 1 (PC1) represents a measure of the overall cytokine secretion ability of a cell and is positively correlated with the intensity of each of the 12 cytokines (Figure S4C). When LT-HSCs, ST-HSCs, MPPs, and LMPPs along with unfractionated LSK cells and total bone marrow (BM) were compared along PC1, a majority of LT-HSCs and LMPPs were clustered at the lower end of PC1, indicating very low overall cytokine secretions, while ST-HSCs and MPPs contained a large fraction of high cytokine secretors (Figure 2D). Principal component 2 (PC2) is a measure of cytokine secretion bias and is positively correlated with lymphoid cytokines (Figure S4D) but negatively correlated with myeloid cytokines (Figure S4E). When the 6 cell types were compared along PC2, LSK cells, ST-HSCs and MPPs were heterogeneous with relatively even distribution across PC2, indicating that they contained a mixture of non-producers, myeloid cytokine-biased, lymphoid cytokine-biased and balanced producers. In comparison, unfractionated BM cells showed moderate myeloid-cytokine bias and LMPPs showed moderate lymphoid-cytokine bias (Figure 2E). It is known that HSCs defined by current best cell surface markers represent a heterogeneous population with biased myeloid or lymphoid lineage potential (Beerman et al., 2010; Challen et al., 2010; Copley et al., 2012). A recent study using a single cell barcode technology also demonstrated the highly heterogeneous nature of the LMPP population (Naik et al., 2013). To add to the complexity, we have now shown that ST-HSCs and MPPs contain heterogeneous subsets based on their cytokine secretion profile. It is reasonable to speculate that the skewed cytokine production ability of ST-HSCs and MPPs may also reflect a biased lineage potential. Unfortunately, the current chip design does not allow us to recover the various cell subsets based on their

NIH-PA Author Manuscript

NIH-PA Author Manuscript

NIH-PA Author Manuscript

cytokine secretion profile for functional and lineage potential analysis. The possible relationship between the heterogeneous cytokine production ability and their lineage potential and functional capacity represents a future direction for research.

Regulation of HSPC cytokine production by NF-κB

NF-κB is a family of transcription factors central to the regulation of inflammation and immune cell activation. Almost three decades of research has elucidated many key physiological functions of NF-κB in innate and adaptive immune cells as well as its involvement in the pathogenesis of many immunological diseases (Baltimore, 2011). However, much less is known about the physiological function of NF-κB in HSPCs during inflammation. Because both LPS and Pam3CSK4 can activate NF-κB, which in turn can upregulate the transcription of many inflammatory cytokines in mature immune cells, we suspected that NF-κB might also regulate cytokine production in HSPCs. To test this, we first determined whether the important components of the TLR/NF-κB pathway were expressed at the protein level in HSPCs. Using a transgenic mouse that has a knock-in of a RELA-GFP fusion protein at the endogenous locus (De Lorenzi et al., 2009), we found that all LT-HSCs and LSK cells were GFP^+, indicating that all HSPCs express RELA (also known as p65) protein, a key subunit of NF-κB (Figure 3A). We then showed that both TLR-2 and TLR-4 receptors were expressed on the surface of LSK cells, with a subset of them expressing both receptors (Figure 3B), a finding consistent with previous reports (Nagai et al., 2006). Next, we asked whether HSPCs have functional NF-κB activity upon TLR stimulation. To study this, we took advantage of a different transgenic NF-κB-GFP reporter mouse, one with GFP expression under the control of the NF-κB regulatory elements (Magness et al., 2004). LPS stimulation *in vivo* upregulated GFP expression from 8% basally to 35-40% in both LSK cells and LT-HSCs (Figure 3C and 3D). More directly, when purified LSK cells and LT-HSCs were stimulated with LPS and Pam3CSK4 *in vitro*, NF-κB activation was again evident by both percent of GFP^+ cells and mean fluorescence intensity (MFI) (Figure 3E and 3F). These results demonstrate that both LSK cells and LT-HSCs contain functional TLR/NF-κB signaling that can be directly activated by TLR-4 and TLR-2 ligands.

To determine whether NF-κB regulates cytokine production in LSK cells, we took advantage of mice deleted for genes important to the NF-κB pathway. NFKB1 (also known as p50) is one of the main subunits of the NF-κB family of transcription factors and p50 deficiency results in defective NF-κB activity in various immune cells (Sha et al., 1995). In contrast, miR-146a is an important negative regulator of NF-κB activation by targeting its upstream signaling transducers TRAF6 and IRAK1. Thus, deficiency in miR-146a leads to enhanced NF-κB activity (Boldin et al., 2011; Zhao et al., 2011; Zhao et al., 2013). When we subjected LSK cells from *Nfkb1*$^{-/-}$ mice (p50 KO) and *Mir146a*$^{-/-}$ mice (miR KO) to the single cell chip analysis, we found that production of all 12 cytokines was significantly attenuated in p50 KO LSK cells and enhanced in miR KO LSK cells, compared to wild type (WT) LSK cells (Figure 4A-C and S3). While 37.9% of WT LSK cells produced cytokines under co-stimulation, the percentage rose to an impressive 69.7% in miR KO and dropped to a mere 2.4% in p50 KO LSK cells (Figure 4A). Furthermore, the percentage of cytokine-producing LSK cells in *Mir146a*$^{-/-}$ *Nfkb1*$^{-/-}$ (miR/p50 DKO) mice was less than in WT

NIH-PA Author Manuscript

NIH-PA Author Manuscript

NIH-PA Author Manuscript

mice, indicating that the lack of p50 is dominant over miR-146a-deficiency (Figure 4A-C and S3). In addition to the percentage of responding cells, the amount of cytokines produced on a per cell basis was also enhanced in miR KO LSK cells and reduced in p50 LSK cells for all the pro-inflammatory cytokines (Figure 4B). These data demonstrate that cytokine production in LSK cells is regulated by the level of NF-κB activity. Tuning the NF-κB activity up or down is sufficient to increase or decrease the cytokine production of LSK cells in response to TLR stimulation. We also measured the co-production of any two cytokines at the single cell level (Figure 4D and 4E). Correlation coefficients (r values) were calculated for all cytokine pairs for WT, p50 KO and miR KO LSK cells, with higher r-values indicating tighter co-regulation. In general, WT LSK cells showed higher correlation coefficients than either p50 KO or miR KO LSK cells, indicating a better co-regulation of these cytokines (Figure 4E, green blocks). This may be functionally important as many of these cytokines are often produced together by a single cell, e.g. myeloid cells produce TNF-α, IL-6 and IL-12 during an inflammatory response, and CD4 T_H1 cells produce IL-2 and IFN-γ. Imbalance in cytokine levels could lead to undesired effects and pathologies. When we performed a principal component analysis on LSK cells of all genotypes, a myeloid cytokine group including IL-6, TNF-α, IL-1β and GM-CSF and a lymphoid cytokine group including IL-2, IL-4 and IL-17a were again identified (Figure 4F). Plotting the measurements onto the dominant 2-dimensional principal component space revealed diminished production of both groups of cytokines in p50 KO LSK cells and enhanced production in miR KO LSK cells. Interestingly, enhancement in the myeloid component was even more prominent in miR KO LSK cells, suggesting miR-146a-deficient LSK cells have especially enhanced myeloid cytokine production. Overall, these results demonstrate that TLR stimulation-mediated cytokine production in HSPCs is exquisitely regulated by the level of NF-κB activity.

Functional significance of HSPC-produced cytokines in regulating myelopoiesis *in vitro*

Cytokines produced by HSPCs are also produced by mature immune cells in the bone marrow and periphery. However, we hypothesize that the location of HSPCs in the stem cell niche may represent an inherent advantage, allowing HSPC-produced cytokines to efficiently regulate their own fate in a more timely fashion during an infection or inflammatory challenge. To assess the functional significance of HSPC-produced cytokines, we first compared the cytokine production capacity of LSK cells with that of more differentiated progenitor cells and mature immune cells. To this end, purified LSK cells and lineage-committed progenitor cells (Lineage$^-$cKit$^+$Sca1$^-$ and Lineage$^-$cKit$^-$Sca1$^+$) from bone marrow as well as CD11b$^+$ myeloid cells, CD4$^+$ T cells, CD8$^+$ T cells and B220$^+$ B cells from spleen were stimulated with LPS plus Pam3CSK4 for 24 hours. Culture medium was then collected for multiplexed ELISA to measure a panel of 15 cytokines. Surprisingly, in the absence of survival and proliferative advantage after stimulation (Figure S5A), LSK cells produced far more cytokines in both quantity and breadth than mature myeloid and lymphoid cells in 24 hours with LPS/Pam3CSK4 stimulation. More impressively, even with much stronger stimuli, such as CpG, anti-CD3/anti-CD28, or 100-fold more LPS, T cells, B cells and myeloid cells were still significantly less potent cytokine-producers than LSK cells (Figure 5A). In addition, LSK cells produced a wide range of myeloid and lymphoid

NIH-PA Author Manuscript

NIH-PA Author Manuscript

NIH-PA Author Manuscript

cytokines, while mature myeloid cells and lymphocytes showed narrower cytokine production profile.

We next determined whether the cytokines produced by HSPCs are able to influence hematopoiesis *in vitro*. We first showed that a fraction of LT-HSCs, LSK cells and myeloid progenitor cells expressed various cytokine receptors, including IL-6Rα, IFN-γR, TNF-R1 and TNF-R2, on their surfaces (Figure S6A). This is consistent with previous studies that provided direct and indirect evidence of cytokine receptor expression in HSPCs (Baldridge et al., 2010; Baldridge et al., 2011; Maeda et al., 2009; Pronk et al., 2011). We next measured myeloid differentiation of LSK cells under LPS/Pam3CSK4 stimulation. Using anti-IL-6 neutralizing antibody, we were able to determine the effect of taking away IL-6 produced by LSK cells on myelopoiesis (Figure 5B and 5C). Interestingly, compared to the isotype antibody control, neutralization of IL-6 had a significant effect on myeloid differentiation. Specifically, the percent of $CD11b^+$ cells produced from LSK cells decreased by about 50% and the number of $CD11b^+$ cells showed a 2-fold reduction over a 4-day period (Fig 5B and 5C). To extend the study to include several other abundantly produced cytokines, we found that neutralization of TNF-α or GM-CSF, but not IFN-γ, also had an inhibitory effect on the generation of myeloid cells (Figure 5D and 5E). Interestingly, neutralization of IL-6, IFN-γ or GM-CSF all decreased the number of LSK cells, suggesting that these cytokines produced by LSK cells have a positive effect on their own proliferation and/or survival (Figure 5E). It is worth noting that we have previously shown that IL-6 can directly induce LSK cell proliferation by BrdU incorporation (Zhao et al., 2013). To further demonstrate the functional importance of HSPC-produced cytokines, we compared cytokines produced by bone marrow cells that were depleted of HSPCs to that of total bone marrow cells in inducing myelopoiesis. To this end, we stimulated equal number of total bone marrow cells and Sca1-depleted bone marrow cells with LPS/Pam3CSK4 *in vitro* for 24 hours and then used the conditioned media to stimulate LSK cells. We saw up to 40% reduction in the number $CD11b^+$ myeloid cells after only 2 days of incubation with conditioned medium from Sca1-depleted bone marrow cells (Figure 5F). This suggests that HSPCs, accounting for less than 1% of total bone marrow cells, make a significant contribution to the cytokine milieu with stimulatory effect on myelopoiesis. Instead of depleting cytokine, we next asked whether increased cytokine production by LSK cells could enhance myelopoiesis. To this end, we used miR-146a-deficient LSK cells that showed exaggerated cytokine production (Figure 4). Purified LSK cells from WT or miR KO mice were stimulated with LPS/Pam3CSK4 *in vitro* for 24 hours and then the conditioned media were used to stimulate newly purified WT LSK cells. After 2 days, we saw a modest but consistent increase in numbers of both LSK cells and $CD11b^+$ cells when WT LSK cells were cultured with miR KO LSK cell-conditioned medium, compared to with WT LSK cell-conditioned medium (Figure 5G). This suggests that with just 24 hours of cytokine accumulation, the exaggerated cytokine production by miR KO LSK cells is sufficient to support enhanced myelopoiesis and LSK cell proliferation/survival. Consistent with this *in vitro* finding, miR KO mice exhibit a significant myeloproliferative disease after chronic inflammatory stimulation as a result of enhanced HSPC proliferation and myeloid differentiation, while deleting IL-6 in miR KO mice effectively ameliorates the myeloproliferative condition (Zhao et al., 2013). Complementing our previous reports that

NIH-PA Author Manuscript

NIH-PA Author Manuscript

NIH-PA Author Manuscript

have shown the involvement of hyperactivated T cells and myeloid cells in miR-146a-deficiency mediated pathologies (Zhao et al., 2011; Zhao et al., 2013), this study shows that exaggerated cytokine production by miR-146a-deficient HSPCs is also a contributor to the enhanced myelopoiesis in miR-146a KO mice.

Functional significance of HSPC-produced cytokines in regulating myelopoiesis *in vivo*

In addition to *in vitro* functional significance, we next determined whether HSPC-produced cytokines are important in regulating hematopoiesis *in vivo*. Because current technology does not allow us to delete a cytokine specifically and selectively in stem and progenitor cells while allowing cytokine production in mature cells, to overcome this hurdle, we have created leucopenic conditions *in vivo* in which mature myeloid and lymphoid cells are severely depleted while stem and progenitor cells are preserved. We created these conditions in mice by injecting chemotherapeutic drug, 5-flurouracil (5-FU), (Figure 6A-C) or by transplanting stem and progenitor cells after lethal irradiation (Figure 6D-F). LPS was injected into mice to stimulate myelopoiesis when neutropenia became the most severe as measured by periodic sampling of peripheral blood. 5-FU is a chemotherapeutic drug that induces significant reduction in mature cells in both bone marrow and periphery while stimulating stem and progenitor cells to cycle (Harrison and Lerner, 1991). After 5-FU injection, myeloid cells started to decline and by day 5, 80% of myeloid cells were depleted in WT, miR-146a KO, IL-6 KO, and miR-146a/IL-6 DKO mice (Figure 6A). At this time, low dose LPS was injected to stimulate myelopoiesis. Consistent with *in vitro* studies, IL-6 KO mice showed a 2-fold decrease in $CD11b^+$ and $Gr1^+$ myeloid cells while miR KO mice showed a modest increase, compared to WT mice (Figure 6B and 6C). In addition, DKO mice showed a similar level of reduction as IL-6 KO mice, indicating that loss of IL-6 is the dominant factor. To perform stem cell transplant, 500,000 purified Lin^-cKit^+ cells from WT, miR KO, IL-6 KO or miR/IL-6 DKO mice were injected into lethally irradiated WT recipient mice. Six days after irradiation and cell injection, all four groups of mice showed severe leucopenia with approximately 8,000 myeloid cells and 20,000 total white blood cells left in the peripheral blood. This represented less than 1% of the normal level and 4% of the number of transplanted HSPCs (Figure 6D-F). LPS stimulation promoted myelopoiesis that was mildly increased in mice receiving miR KO HSPCs, but was significantly attenuated in mice receiving IL-6 KO or miR/IL-6 DKO HSPCs, indicating that IL-6 produced by HSPCs is an important factor in promoting myeloid cell recovery during neutropenia (Figure 6D-F). Overall, these *in vivo* experiments show that in mice with severe leucopenia, LPS-stimulated production of cytokines, especially IL-6, by endogenous or transplanted HSPCs has a significant positive impact on stress-induced myelopoiesis.

Within the bone marrow niche, we speculate that the cytokines released by HSPCs upon TLR stimulation can act on themselves or neighboring HSPCs. To further delineate whether HSPC-produced cytokines mediate hematopoiesis predominantly through an autocrine or paracrine fashion, we injected NF-κB-GFP reporter mice with both LPS and BrdU to determine the relationship between cytokine-producing HSPCs and proliferating HSPCs. GFP expression, an indicator of NF-κB activation and cytokine production, and BrdU incorporation, a marker of proliferation, were co-stained in myeloid progenitor cells, LSK cells and LT-HSCs at 4, 12 and 24 hours (Figure 6G). The result showed that LSK cells and

NIH-PA Author Manuscript

NIH-PA Author Manuscript

NIH-PA Author Manuscript

LT-HSCs rapidly turned on NF-κB in response to LPS stimulation, while myeloid progenitor cells went into cycle quickly. As time elapsed, LT-HSCs and LSK cells started to proliferate while NF-κB activity gradually dampened. Interestingly, throughout the stimulation, cells with NF-κB activity and cells that rapidly proliferated represented two largely non-overlapping populations in all the stem and progenitor subsets. While this result has multiple potential interpretations, the fact that we have been unable to capture a large fraction of cells that are simultaneously positive for BrdU and GFP throughout the 24-hour interval suggests to us the following mechanism: LPS-mediated NF-κB activation in HSPCs does not appear to directly turn on a proliferation program, and instead, cytokines are induced which in turn act on cytokine receptors on neighboring HSPCs to stimulate proliferation and differentiation. The nature of this type of paracrine signaling and the distinction between the proliferative and the NF-κB-activated subsets within HSPCs require further investigation.

DISCUSSION

In this study, we have shown that ST-HSCs and MPPs can translate danger signals arising from an infection into cytokine signals that can directly regulate stress-induced hematopoiesis. Significantly, the cytokine production ability of HSPCs trumps both mature myeloid and lymphoid cells in terms of speed, magnitude and breadth. In the bone marrow stem cell niche, this property of HSPCs may play an important role of providing a rapid response time from the encounter of an infection to the output of myeloid cells. In addition to residing in the bone marrow, HSPCs are known to egress from the marrow and traffic through the blood and lymphatic circulation to peripheral organs, including spleen, liver, lymph nodes, gut and adipose tissues, where they may be exposed to a heavy burden of danger signals. These extramedullary sites may provide excellent opportunities for HSPCs to coordinate rapid stress-induced hematopoiesis upon TLR stimulation (Han et al., 2010; Jaiswal and Weissman, 2009; Massberg et al., 2007; Wesemann et al., 2013).

Because all the cytokines produced by HSPCs are also produced by mature immune cells and some non-hematopoietic cells, to isolate the effect of cytokines produced by HSPCs from mature cells *in vivo* is difficult, if not impossible, given current technical limitations in specifically deleting a gene in HSCs while turning it back on in mature cells. Therefore, we have first relied on *in vitro* studies to demonstrate the functional importance of HSPC-produced cytokines in regulating myelopoiesis. Furthermore, by comparing total bone marrow cells with Sca1-depleted bone marrow cells, we have provided evidence that HSPCs can make significant contribution to cytokine-mediated myelopoiesis. In addition, there are situations when mature immune cells are significantly depleted, such as during sepsis, post chemotherapy and during the initial recovering phase of stem cell transplant. During these situations when mature immune cells are depleted and HSPCs are over-represented, the ability of HSPCs to respond to stress directly to produce cytokines may be critical in mediating rapid hematopoietic cell recovery. We have created these situations in mice to mimic neutropenic conditions after chemotherapy or stem cell transplant and have shown that the ability of HSPCs to produce IL-6 is particularly important in mediating stress-induced myelopoiesis. In clinical practice, G-CSF and GM-CSF are used in certain situations after chemotherapy or stem cell transplant to stimulate neutrophil recovery in

NIH-PA Author Manuscript

NIH-PA Author Manuscript

NIH-PA Author Manuscript

neutropenic patients who are susceptible to fatal infection (Bennett et al., 2013). Better understanding of the cytokine-mediated hematopoiesis in neutropenic conditions will provide further insight in potentially more effective hematopoietic-stimulating factors.

In addition to neutropenic conditions, we reason that this stem and progenitor cell property is also important in physiological condition, despite of the rarity of HSPCs among differentiated hematopoietic cells. Firstly, the speed, magnitude and breadth of the cytokine produced by HSPCs in comparison to mature immune cells are impressive. Furthermore, this has not taken into the account the unique location of HSPCs in the stem cell niche. Location and organization of HSPCs within the bone marrow niche have long been appreciated to play an important role in their self-renewal and proliferative properties (Shen and Nilsson, 2012). Perhaps groups of HSPCs residing in close proximity represent a unique advantage for rapid autocrine or paracrine-mediated hematopoiesis. Through BrdU incorporation in NF-κB-GFP reporter mice, we have shown that HSPCs with NF-κB activity and that are actively proliferating are largely two distinct populations. We speculate that a potential paracrine regulatory signaling may be at work within the bone marrow that involves one subset of HSPCs responding to TLR stimulation by rapidly turning on NF-κB and producing copious amount of cytokines and a neighboring cell population with cytokine receptors that can undergo rapid proliferation and differentiation in response to cytokine stimulation. In support of the notion, while some LSK cells express both TLR-4 and IL-6Rα, it appears that a fraction of LSK cells express only the TLR or the cytokine receptor (Figure S6B), suggesting that HSPCs contain heterogeneous subsets with intrinsic difference in their response to TLR and cytokine stimuli.

The questions regarding the extent of involvement of HSPC-produced cytokines in hematopoiesis in non-neutropenic host and the nature of HSPC heterogeneity based on differential cytokine production or TLR/cytokine receptor expression remain open and will be an area of significant interest for future studies. In addition to analyzing stem cell organization within the bone marrow architecture and the function of various HSPC subsets with differential responsiveness to TLR agonists and/or cytokines, we are also currently redesigning the microfluidic platform in order to recover individual cells from the chip after proteomic analysis for subsequent lineage and functional analysis. Furthermore, there are perhaps limitations in the *in vitro* on-chip stimulation, which may not provide the optimal conditions for culturing undifferentiated HSPCs. This may result in a reduction in the cells' functional robustness and an under-estimate of the true percentage of cytokine-producing cells *in vivo*, despite our post stimulation analysis to ensure that HSPCs remain phenotypically undifferentiated by FACS and morphologically intact by microscopy. The ability to recover individual cells post stimulation will allow us to better assess cell viability.

Functions of NF-κB in immune cells have been extensively studied. However, knowledge of the functional role of NF-κB in HSPCs has been limited. In this study, we have connected a known function of NF-κB, the regulation of cytokine production, to two unexpected multipotent hematopoietic cell populations, ST-HSCs and MPPs. What is also intriguing is that some LTHSCs appear able to respond to TLR stimulation by activation of NF-κB and all HSCs appear to have at least the p65 subunit of NF-κB. Thus, despite NF-κB by itself

NIH-PA Author Manuscript

NIH-PA Author Manuscript

NIH-PA Author Manuscript

being insufficient to enable cytokine secretion in LT-HSCs, NF-κB is present from the inception of hematopoiesis and may regulate other aspects of HSC biology.

EXPERIMENTAL PROCEDURES

Animal models

All mice (wildtype, *Nfkb1*$^{-/-}$, *Mir146a*$^{-/-}$, *il6*$^{-/-}$, *Nfkb1*$^{-/-}$*Mir146a*$^{-/-}$, *il6*$^{-/-}$*Mir146a*$^{-/-}$, RELA-GFP knock-in mouse, NF-κB-eGFP reporter mouse) were on a C57BL/6 genetic background and housed under specific pathogen-free condition at the California Institute of Technology. Mice used for all experiments were age-and-sex-matched 6-8 week-old female mice. All experiments were approved by the institutional Animal Care and Use Committee of the California Institute of Technology.

FACS sort

6-8 week-old female mice were used in all sorting experiments. In general, 15-20 mice of the same genotype were used for FACS sorting in order to obtain sufficient stem and progenitor cells. Bone marrow cells were first subjected to magnetic bead selection (Miltenyi) according to manufacturer's protocol to deplete lineage positive cells and then sorted on a BD FACS Aria sorter at the Caltech FACS Core. More details can be found in the Supplemental Experimental Procedures section.

Single cell cytokine chip analysis

We integrated upstream FACS purification techniques with the single cell barcode chip to study the functional proteomics from phenotypically defined single cells. The chips used in this study have >5000 microchambers of about 100 picoliters each in size to enable sensitive detection of proteins. Within each microchamber, a panel of 12 cytokines (TNF-α, GM-CSF, IL-6, IL-12p40, IFN-γ, IL-2, IL-4, IL-10, TGF-β1, CCL-2, IL-17A and IL-1β) can be simultaneously measured by a sandwich ELISA-like assay. The manufacture procedure of the chip has been described in our previous study (Ma et al., 2011) and the detailed experimental steps can be found in the Supplemental Experimental Procedures section. Briefly, FACS-purified cells were cultured at 37 degree in 5% CO_2 cell incubator with medium alone, medium plus LPS, or medium plus LPS and Pam3CSK4 for 12 hours. At the end of stimulation, the chip was imaged using high resolution bright field microscope. Cell number in each chamber was counted and cell viability was assessed to exclude fragmented or non-light reflective cells blindly by trained personnel. Then cells were washed off and the chips were developed via an immuno-sandwich assay. GenePix 4400A microarray scanner was used to scan slides and data were analyzed with GenePix Pro 7 software. Each single cell barcode chip analysis of a specific cell subset, genotype, and stimulating condition was performed at least two times.

Mutliplexed cytokine analysis of bulk cell culture medium

For multiplexed cytokine analysis of bulk cell culture medium, 100,000 cells of each FACS-purified subset were stimulated in 100μl medium with various stimulations for 24 hours in a 96-well plate. The medium was then collected and concentrated by 4-fold before subjected to multiplexed ELISA quantification of 15 different cytokines and chemokines. For

NIH-PA Author Manuscript

NIH-PA Author Manuscript

NIH-PA Author Manuscript

multiplexed ELISA quantification, the detection method is identical to the single cell chip analysis described above. The difference is the sample here consists of culturing medium only. Briefly, the ELISA chip was first blocked with 3% BSA/PBS buffer. Then was hybridized with an antibody-ssDNA conjugate cocktail and washed with 3% BSA/PBS, followed by applying medium sample. The assay was completed by applying secondary biotinylated antibodies, streptavidin-cy3 in sequence. Every step takes an hour. Finally, the slide was washed with 3% BSA/PBS, 50%/50% PBS/DI water and water in sequence before spin dried and scanned with a GenePix 4400A microarray scanner. Mutiplexed cytokine analysis of a specific cell subset, genotype, and stimulating condition was performed at least two times.

In vitro analysis of myeloid differentiation

For analysis of myeloid differentiation under cytokine neutralizing antibodies, sorted LSK cells (15,000 cells per 100μl medium) were stimulated with LPS (100ng/ml), Pam3CSK4 (1μg/ml) and SCF (50ng/ml), in the presence of various cytokine neutralizing antibodies. Antibody concentrations used were isotype control (1μg/ml), anti-IFN-γ (1μg/ml), anti-IL-6 (1μg/ml), anti-GM-CSF (5μg/ml) and anti-TNF-α (5μg/ml) (eBioscience). Control, isotype antibody control; all Abs, a combination of anti-IL-6, anti-IFN-γ, anti-GM-CSF and anti-TNF-α neutralizing antibodies. Cells were analyzed on Day 3 by FACS for percent and number of myeloid cells and LSK cells. For analysis of myeloid differentiation under conditioned medium, WT or miR-146a KO LSK cells (30,000 cells per 100μl medium) were stimulated with LPS (100ng/ml) and Pam3CSK4 (1μg/ml) for 24 hours to induce cytokine production into the culturing medium. The culturing medium from either WT or miR KO LSK cells was then collected and used to stimulate freshly purified WT LSK cells. Number of myeloid and LSK cells was analyzed after 2 days by FACS. All experiments were performed two times with three biological replicates, each of which was sorted from pooled bone marrow cells of 6-10 mice.

In vivo analysis of myeloid differentiation

For 5-fluorouracil-induced leucopenia, WT, miR-146a KO, IL-6 KO and miR-146a/IL-6 DKO mice were injected with 5-fluorouracil (5-FU) (250 mg/kg of body weight, i.p.) (Sigma). Peripheral blood was obtained on Day 0, 2, 4, and 5 for FACS analysis to determine the severity of neutropenia. On Day 5, LPS (0.3 mg/kg of body weight, i.p.) was injected and mice were bled 24 hours later for FACS analysis. For stem cell transplant study after lethal irradiation, $Lin^{-}cKit^{+}$ cells were purified from the bone marrow of WT, miR-146a KO, IL-6 KO and miR-146a/IL-6 DKO mice. 500,000 cells were injected intravenously into each lethally irradiated (1000 rad in one dose) WT recipient mouse. On Day 6, mice were bled for FACS analysis and LPS injection (0.3 mg/kg of body weight, i.p.) was given; 48 hours later, mice were bled again for FACS analysis. Data represent cumulative results from 2 independent mouse experiments.

Computational algorithm and statistical analysis

In Figure 3 and 5, F-tests were used to compare variances and then the appropriate two-sided student t-tests were applied. For all figures with error bars, they were graphed as mean +/− standard error of the mean (s.e.m.); for all heatmaps, scale bars were presented as mean

NIH-PA Author Manuscript

NIH-PA Author Manuscript

NIH-PA Author Manuscript

+/− standard deviation (s.d.). * indicates $p < 0.05$; ** indicates $p < 0.01$; *** indicates $p < 0.001$.

For all single cell cytokine chip analysis, custom written software routines in R language were used to process, analyze and visualize the single cell functional assay results. Briefly, the algorithm converts raw fluorescence images into numerical fluorescence intensity values for each assayed protein within a given microchamber, matched with the number of cells. Number of cells within each microchamber was determined manually by microscopy. The average background signal levels from all 0-cell microchambers were used to set the gate to separate non-producing cells from cytokine-producing cells. Detailed statistical analysis method for principal component analysis (Figure 1D, 2D, 2F and 4F) can be found in the Supplemental Experimental Procedures section and our previous publication (Ma et al., 2011). This type of statistical analysis and graphical representations are routinely used to analyze large-scale multidimensional dataset from numerous cell subsets (Bendall et al., 2011).

Supplementary Material

Refer to Web version on PubMed Central for supplementary material.

Acknowledgments

The authors wish to thank Caltech animal facility, flow cytometry core facility and Drs. Alejandro Balazs, Devdoot Majumdar and Michael Bethune of the Baltimore Lab for their help. RELA-GFP knock-in mouse and NF-κB-eGFP reporter mouse were obtained from Dr. Manolis Pasparakis of University of Cologne and Dr. Christian Jobin of University of North Carolina, respectively. The work was supported by research grants R01AI079243 (DB), R01CA170689 (JRH), National Research Service Award F30HL110691 (JLZ), UCLA/Caltech Medical Scientist Training Program (JLZ and AM), Rosen Fellowship (CM), NIH New Innovator Award DP2GM111099 (RMO), the Pathway to Independence Award R00HL102228 (RMO), and American Cancer Society Research Grant (RMO), with core facilities support from 5U54CA119347 (JRH).

REFERENCES

Adolfsson J, Mansson R, Buza-Vidas N, Hultquist A, Liuba K, Jensen CT, Bryder D, Yang L, Borge OJ, Thoren LA, et al. Identification of Flt3+ lympho-myeloid stem cells lacking erythro-megakaryocytic potential a revised road map for adult blood lineage commitment. Cell. 2005; 121:295–306. [PubMed: 15851035]

Baldridge MT, King KY, Boles NC, Weksberg DC, Goodell MA. Quiescent haematopoietic stem cells are activated by IFN-gamma in response to chronic infection. Nature. 2010; 465:793–797. [PubMed: 20535209]

Baldridge MT, King KY, Goodell MA. Inflammatory signals regulate hematopoietic stem cells. Trends Immunol. 2011; 32:57–65. [PubMed: 21233016]

Baltimore D. NF-kappaB is 25. Nat Immunol. 2011; 12:683–685. [PubMed: 21772275]

Beerman I, Bhattacharya D, Zandi S, Sigvardsson M, Weissman IL, Bryder D, Rossi DJ. Functionally distinct hematopoietic stem cells modulate hematopoietic lineage potential during aging by a mechanism of clonal expansion. Proc Natl Acad Sci U S A. 2010; 107:5465–5470. [PubMed: 20304793]

Bendall SC, Simonds EF, Qiu P, Amir el AD, Krutzik PO, Finck R, Bruggner RV, Melamed R, Trejo A, Ornatsky OI, et al. Single-cell mass cytometry of differential immune and drug responses across a human hematopoietic continuum. Science. 2011; 332:687–696. [PubMed: 21551058]

Bennett CL, Djulbegovic B, Norris LB, Armitage JO. Colony-stimulating factors for febrile neutropenia during cancer therapy. N Engl J Med. 2013; 368:1131–1139. [PubMed: 23514290]

NIH-PA Author Manuscript

NIH-PA Author Manuscript

NIH-PA Author Manuscript

Boldin MP, Taganov KD, Rao DS, Yang L, Zhao JL, Kalwani M, Garcia-Flores Y, Luong M, Devrekanli A, Xu J, et al. miR-146a is a significant brake on autoimmunity, myeloproliferation, and cancer in mice. J Exp Med. 2011; 208:1189–1201. [PubMed: 21555486]

Challen GA, Boles NC, Chambers SM, Goodell MA. Distinct hematopoietic stem cell subtypes are differentially regulated by TGF-beta1. Cell Stem Cell. 2010; 6:265–278. [PubMed: 20207229]

Copley MR, Beer PA, Eaves CJ. Hematopoietic stem cell heterogeneity takes center stage. Cell Stem Cell. 2012; 10:690–697. [PubMed: 22704509]

De Lorenzi R, Gareus R, Fengler S, Pasparakis M. GFP-p65 knock-in mice as a tool to study NF-kappaB dynamics in vivo. Genesis. 2009; 47:323–329. [PubMed: 19263497]

Essers MA, Offner S, Blanco-Bose WE, Waibler Z, Kalinke U, Duchosal MA, Trumpp A. IFNalpha activates dormant haematopoietic stem cells in vivo. Nature. 2009; 458:904–908. [PubMed: 19212321]

Forsberg EC, Serwold T, Kogan S, Weissman IL, Passegue E. New evidence supporting megakaryocyte-erythrocyte potential of flk2/flt3+ multipotent hematopoietic progenitors. Cell. 2006; 126:415–426. [PubMed: 16873070]

Han J, Koh YJ, Moon HR, Ryoo HG, Cho CH, Kim I, Koh GY. Adipose tissue is an extramedullary reservoir for functional hematopoietic stem and progenitor cells. Blood. 2010; 115:957–964. [PubMed: 19897586]

Harrison DE, Lerner CP. Most primitive hematopoietic stem cells are stimulated to cycle rapidly after treatment with 5-fluorouracil. Blood. 1991; 78:1237–1240. [PubMed: 1878591]

Jaiswal S, Weissman IL. Hematopoietic stem and progenitor cells and the inflammatory response. Ann N Y Acad Sci. 2009; 1174:118–121. [PubMed: 19769744]

Janeway, CA., Jr; Travers, P.; Walport, M.; Shlomchik, MJ. Cytokines and Their Receptors. 5th edn. Garland Science; New York: 2001. Immunobiology: The Immune System in Health and Disease. Appendix III..

King KY, Goodell MA. Inflammatory modulation of HSCs: viewing the HSC as a foundation for the immune response. Nat Rev Immunol. 2011; 11:685–692. [PubMed: 21904387]

Ma C, Fan R, Ahmad H, Shi Q, Comin-Anduix B, Chodon T, Koya RC, Liu CC, Kwong GA, Radu CG, et al. A clinical microchip for evaluation of single immune cells reveals high functional heterogeneity in phenotypically similar T cells. Nat Med. 2011; 17:738–743. [PubMed: 21602800]

Maeda K, Malykhin A, Teague-Weber BN, Sun XH, Farris AD, Coggeshall KM. Interleukin-6 aborts lymphopoiesis and elevates production of myeloid cells in systemic lupus erythematosus-prone B6.Sle1.Yaa animals. Blood. 2009; 113:4534–4540. [PubMed: 19224760]

Magness ST, Jijon H, Van Houten Fisher N, Sharpless NE, Brenner DA, Jobin C. In vivo pattern of lipopolysaccharide and anti-CD3-induced NF-kappa B activation using a novel gene-targeted enhanced GFP reporter gene mouse. J Immunol. 2004; 173:1561–1570. [PubMed: 15265883]

Massberg S, Schaerli P, Knezevic-Maramica I, Kollnberger M, Tubo N, Moseman EA, Huff IV, Junt T, Wagers AJ, Mazo IB, von Andrian UH. Immunosurveillance by hematopoietic progenitor cells trafficking through blood, lymph, and peripheral tissues. Cell. 2007; 131:994–1008. [PubMed: 18045540]

Megias J, Yanez A, Moriano S, O'Connor JE, Gozalbo D, Gil ML. Direct Toll-like receptor-mediated stimulation of hematopoietic stem and progenitor cells occurs in vivo and promotes differentiation toward macrophages. Stem Cells. 2012; 30:1486–1495. [PubMed: 22511319]

Mossadegh-Keller N, Sarrazin S, Kandalla PK, Espinosa L, Stanley ER, Nutt SL, Moore J, Sieweke MH. M-CSF instructs myeloid lineage fate in single haematopoietic stem cells. Nature. 2013; 497:239–243. [PubMed: 23575636]

Nagai Y, Garrett KP, Ohta S, Bahrun U, Kouro T, Akira S, Takatsu K, Kincade PW. Toll-like receptors on hematopoietic progenitor cells stimulate innate immune system replenishment. Immunity. 2006; 24:801–812. [PubMed: 16782035]

Naik SH, Perie L, Swart E, Gerlach C, van Rooij N, de Boer RJ, Schumacher TN. Diverse and heritable lineage imprinting of early haematopoietic progenitors. Nature. 2013; 496:229–232. [PubMed: 23552896]

NIH-PA Author Manuscript

NIH-PA Author Manuscript

NIH-PA Author Manuscript

Pronk CJ, Veiby OP, Bryder D, Jacobsen SE. Tumor necrosis factor restricts hematopoietic stem cell activity in mice: involvement of two distinct receptors. J Exp Med. 2011; 208:1563–1570. [PubMed: 21768269]

Sha WC, Liou HC, Tuomanen EI, Baltimore D. Targeted disruption of the p50 subunit of NF-kappa B leads to multifocal defects in immune responses. Cell. 1995; 80:321–330. [PubMed: 7834752]

Shen Y, Nilsson SK. Bone, microenvironment and hematopoiesis. Curr Opin Hematol. 2012; 19:250–255. [PubMed: 22504524]

Wesemann DR, Portuguese AJ, Meyers RM, Gallagher MP, Cluff-Jones K, Magee JM, Panchakshari RA, Rodig SJ, Kepler TB, Alt FW. Microbial colonization influences early B-lineage development in the gut lamina propria. Nature. 2013; 501:112–115. [PubMed: 23965619]

Zhao JL, Rao DS, Boldin MP, Taganov KD, O'Connell RM, Baltimore D. NF-kappaB dysregulation in microRNA-146a-deficient mice drives the development of myeloid malignancies. Proc Natl Acad Sci U S A. 2011; 108:9184–9189. [PubMed: 21576471]

Zhao JL, Rao DS, O'Connell RM, Garcia-Flores Y, Baltimore D. MicroRNA-146a acts as a guardian of the quality and longevity of hematopoietic stem cells in mice. Elife. 2013; 2:e00537. [PubMed: 23705069]

NIH-PA Author Manuscript

NIH-PA Author Manuscript

NIH-PA Author Manuscript

HIGHLIGHTS

- Undifferentiated HSPCs produce a wide range of cytokines upon stimulation.
- The cytokine production function of HSPCs is regulated by the TLR/NF-κB axis.
- HSPCs are significantly more potent cytokine secretors than mature immune cells.
- Cytokines produced by HSPCs allow efficient myelopoiesis *in vitro* and *in vivo*.

NIH-PA Author Manuscript

NIH-PA Author Manuscript

NIH-PA Author Manuscript

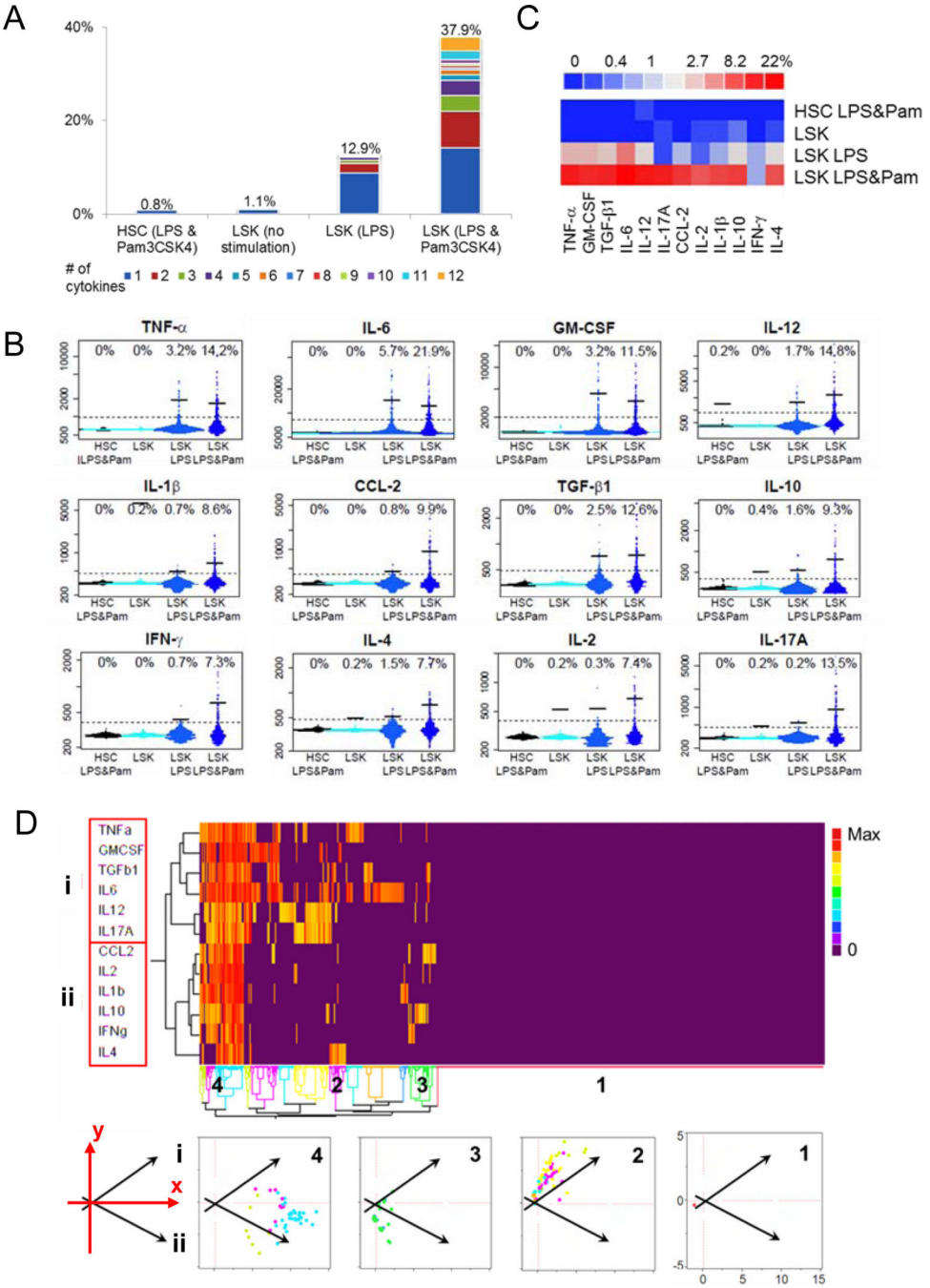

Figure 1. Single cell analysis of cytokine production by WT HSPCs in response to TLR stimulation (see also Figure S1-3)

A-D are from single cell cytokine chip analysis. The four cell groups analyzed are HSCs with LPS and Pam3CSK4, LSK cells with medium only, LSK cells with LPS, and LSK cells with LPS and Pam3CSK4 stimulation for 12 hours. LSK is defined by Lineage^{-}Sca1^{+}cKit^{+} and HSC is defined by LSK CD150^{+}CD48^{-}. A. Polyfunctionality and populational level statistics of the cell types analyzed. Percentage of cells secreting different number of cytokines is shown for each cell type studied. Different color represents cells producing different number of cytokines from 1 to 12 (labeled with different colors); the number on top

NIH-PA Author Manuscript

NIH-PA Author Manuscript

NIH-PA Author Manuscript

of each cell type shows the total percentage of cells secreting detectable amount of any of the 12 cytokines. B. Comparison of HSCs and LSK cells by individual cytokine. Each plot is composed of several thousand individual dots from several thousand single cells. The four cell groups arranged from left to right are HSC under LPS and Pam3CSK4 stimulation (black), LSK with no stimulation (cyan), LSK with LPS stimulation only (light blue) and LSK with LPS and Pam3CSK4 stimulation (dark blue). The numbers on top represent the percentage of cytokine producing cells identified by the gate (the dotted line) and the bars represent the mean intensity of only the cytokine-producing cells (average intensity of the cells above the dotted line). C. A summary heat map showing the percentage of HSCs and LSK cells that secrete any individual cytokine under different stimulations. D. Clustering analysis of WT LSK cells under LPS and Pam3CSK4 stimulation, with result presented as a heat map and scatter plots. The data is analyzed by two-way hierarchical clustering that groups similar proteins and cells together. The grouping is shown by the tree structure for both proteins and cells. Each row represents an individual cytokine and each column represents an individual cell. The result is presented by a heat map with color representing the amount of cytokine secretion, from purple (undetectable) to yellow (intermediate) to red (maximum). Two major groups of proteins (i and ii) and four main groups of cells (1 to 4) are identified. Each cell group is replotted onto the two-dimensional principal component plane. This reduced space is the one that can explain the largest fraction (65%) of the information from the data. The arrows indicate the directions of the two cytokine functional groups aligned to the x-y axis.

NIH-PA Author Manuscript

NIH-PA Author Manuscript

NIH-PA Author Manuscript

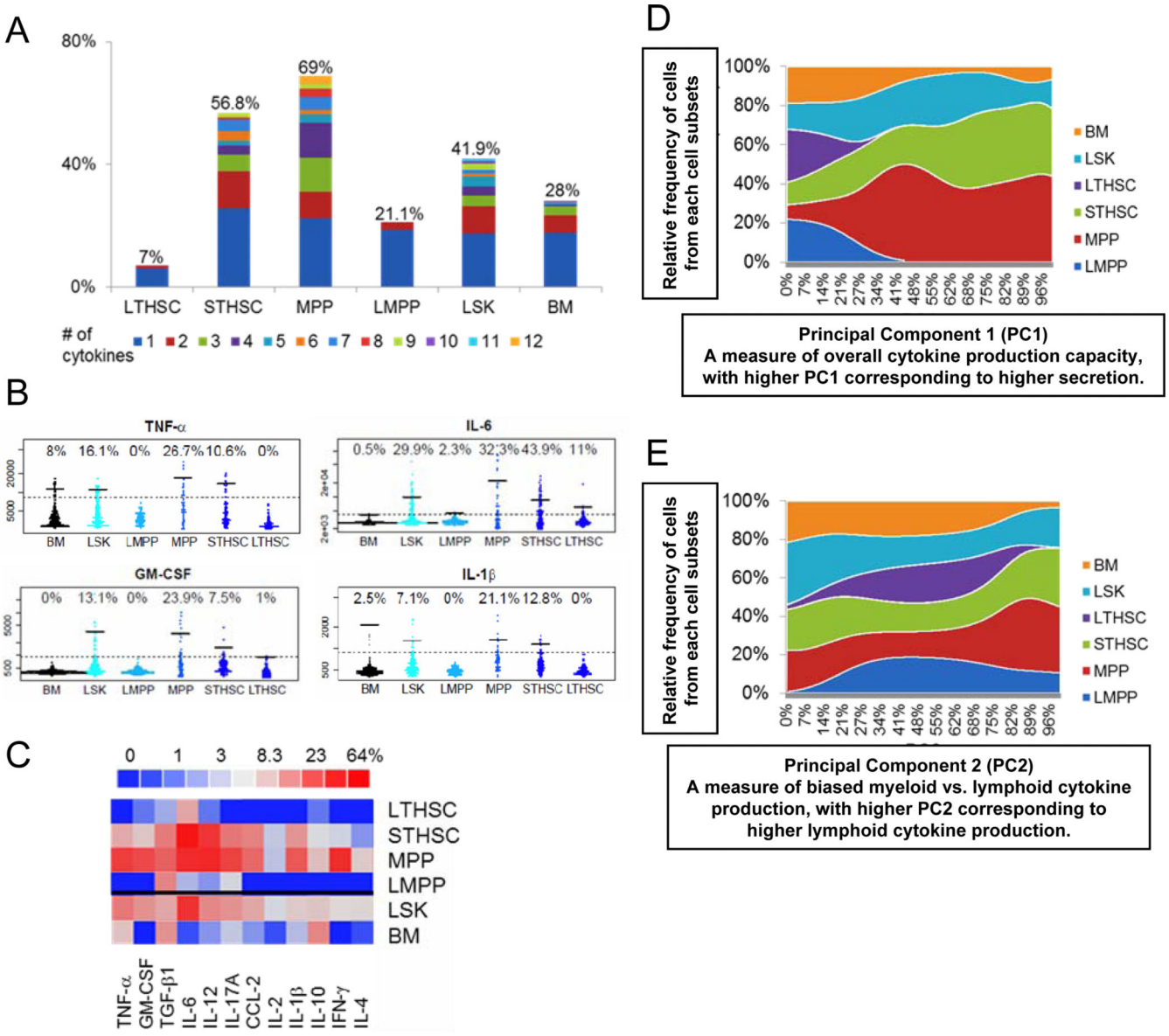

Figure 2. Single cell analysis of cytokine production by various HSPC subsets in response to TLR stimulation (see also Figure S4)

A-E are from single cell cytokine chip analysis. The six cell groups analyzed are BM (total bone marrow cells), LSK cells, LMPPs (LSK CD34^{+}Flt3^{hi}), MPPs (LSK CD34^{+}Flt3^{int}), ST-HSCs (LSK CD34^{+}Flt3^{-}) and LT-HSCs (LSK CD34^{-}Flt3^{-}) all under LPS and Pam3CSK4 stimulation for 12 hours. A. Polyfunctionality and populational level statistics of the cell types analyzed. Percentage of cells secreting different number of cytokines is shown for each cell type studied. Different color represents cells producing different number of cytokines from 1 to 12 (labeled with different colors); the number on top of each cell type represents the total percentage of cells secreting detectable amount of any of the 12 cytokines. B. Comparison of HSPC subsets by individual cytokines. 4 out of 12 cytokines are shown here and the rest is shown in Figure S4B. Each plot is composed of several thousand individual dots from several thousand single cells. The six cell groups arranged

NIH-PA Author Manuscript

NIH-PA Author Manuscript

NIH-PA Author Manuscript

from left to right are Total BM, LSK cells, LMPPs, MPPs, ST-HSCs, LT-HSCs under LPS and Pam3CSK4 stimulation. The numbers on top represent the percentage of cytokine producing cells identified by the gate (the dotted line) and the bars represent the mean intensity of only the cytokine-producing cells (average intensity of the cells above the dotted line). C. A summary heat map showing the percentage of the six groups of cells that secrete any individual cytokine under different stimulations. D and E are principal component analysis of all six cell groups that reduce a 12-dimensional cytokine data set from 6 different cell groups into two principal components (PC1 and PC2) that represent the majority of the information. D. Principal component 1 (PC1) represents the overall cytokine production capacity of a cell and is positively correlated to the overall intensity of all 12 cytokines (see Figure S4C). After all 12 cytokine intensities of each cell are converted into a single PC1 value (as % of the maximal PC1), relative frequency of cells within each PC1 interval is calculated for all 6 cell subsets. D graphs the relative frequency of cells (y-axis) of the six cell groups against %PC1 (x-axis). Each cell type is represented by a different color. E. Principal component 2 (PC2) represents the level of biased cytokine production profile and is positively correlated to the lymphoid group of cytokines, including IL-2, IL-17a, IL-4, IL-12, IL-1β and IFN-γ, but is negatively correlated to the myeloid group of cytokines, including TNF-α, IL-6 and GM-CSF (see Figure S4D and S4E). E graphs the relative frequency of cells (y-axis) of the six cell groups against %PC2 (x-axis). Each cell type is represented by a different color.

NIH-PA Author Manuscript

NIH-PA Author Manuscript

NIH-PA Author Manuscript

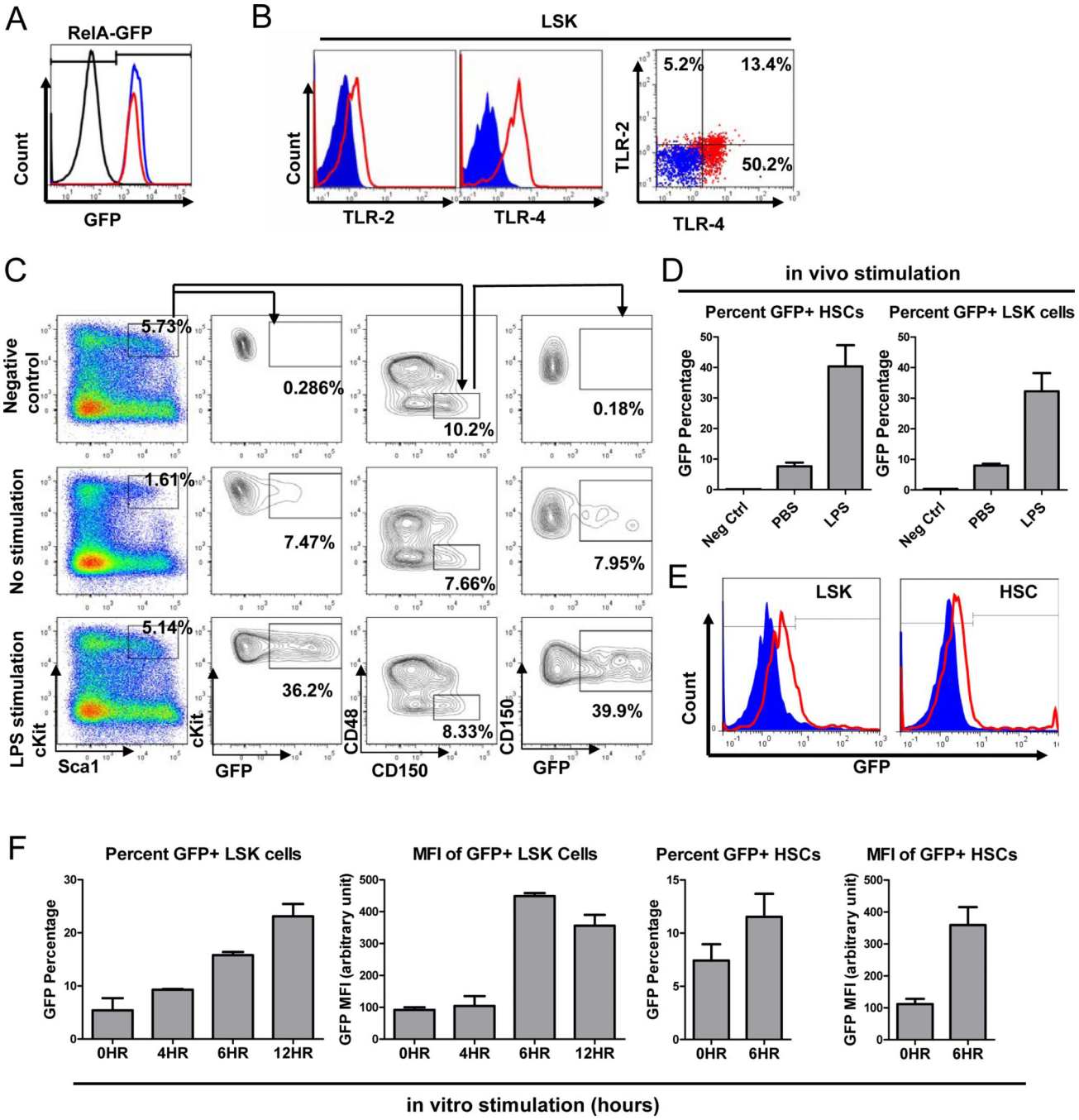

Figure 3. NF-κB activation through TLRs in HSPCs

A-F represent data from FACS analysis. A. Representative FACS histogram of LSK cells (blue) and HSCs (LSK $CD150^{+}CD48^{-}$) (red) from RELA-GFP transgenic mice; LSK cells from a wildtype (WT) C57Bl/6 mouse as a negative control (black). B. Representative FACS plots of TLR-2 and TLR-4 surface expression of WT LSK cells. Blue represents isotype antibody control and red represents fluorescence-conjugated antibodies against TLR-2 (left panel), TLR-4 (middle panel), or both (Right panel). C-F. Determination of TLR/NF-κB functionality in LSK cells and HSCs using mice in which GFP production is

NIH-PA Author Manuscript

NIH-PA Author Manuscript

NIH-PA Author Manuscript

under NF-κB regulatory control. C and D represent experiments from *in vivo* stimulation C. LPS-stimulated WT mouse is used as a negative control (top row) for GFP expression. No stimulation (middle row) corresponds to PBS-treated NF-κB-GFP transgenic reporter mice; LPS stimulation (bottom row) corresponds to LPS-stimulated NF-κB-GFP transgenic reporter mice (2mg/kg body weight LPS for 6 hours). D. Quantification of GFP^+ percentages in LSK cells and HSCs from negative control, unstimulated and LPS-stimulated NF-κB-GFP transgenic reporter mice (n=3). E and F represent experiments from *in vitro* stimulation of purified LSK cells and HSCs. E. Representative FACS histograms of LSK cells and HSCs sorted from NF-κB-GFP transgenic reporter mice. Blue represents unstimulated LSK cells or HSCs and red represents cells stimulated *in vitro* with LPS (100ng/ml) for 6 hours. F. Quantification of GFP^+ percentages and GFP mean fluorescence intensity (MFI) of of LSK cells at 0, 4, 6 and 12 hours and HSCs at 0 and 6 hours (n=3). Data are presented as mean +/− s.e.m.

NIH-PA Author Manuscript

NIH-PA Author Manuscript

NIH-PA Author Manuscript

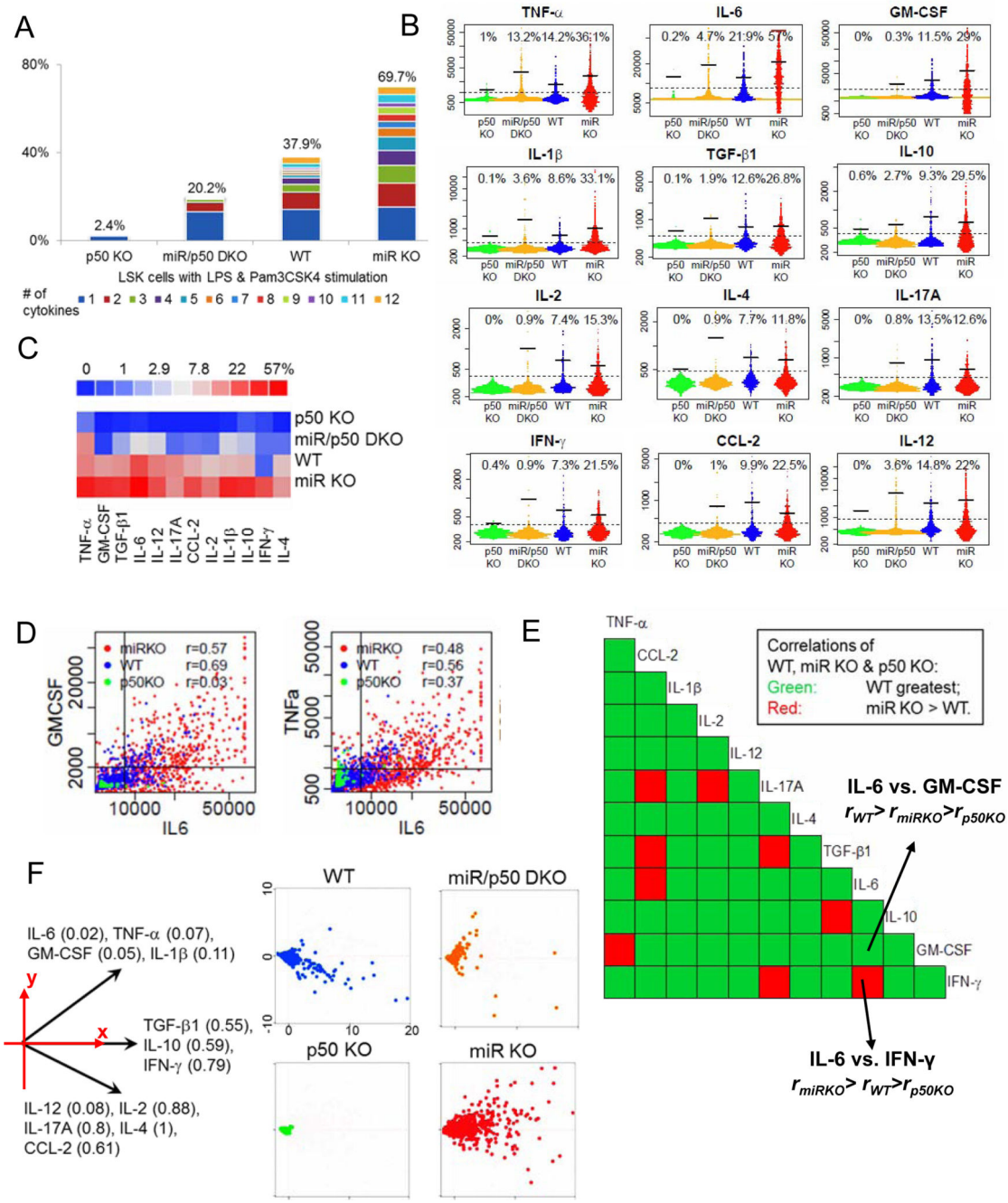

Figure 4. Regulation of HSPC cytokine production by NF-κB (see also Figure S3)

A-F are data from single cell cytokine chip analysis. LSK cells were sorted from wildtype (WT), *Nfkb1*$^{-/-}$ (p50 KO), *Mir146a*$^{-/-}$ (miR KO), and *Nfkb1*$^{-/-}$*Mir146a*$^{-/-}$ (miR/p50 DKO) mice and were stimulated with LPS and Pam3CSK4 for 12 hours. A. Polyfunctionality and population level statistics of LSK cells of different genetic models. Percentage of LSK cells secreting different number of cytokines is shown for each cell type studied. Different color represents cells producing different number of cytokines from 1 to 12 (labeled by different colors); the number on top of each cell type represents the total percentage of cells secreting

NIH-PA Author Manuscript

NIH-PA Author Manuscript

NIH-PA Author Manuscript

detectable amount of any cytokine. B. Comparison of the cytokine secretion capacity of LSK cells from different genetic models. Each plot represents cytokine intensity scatter plots for a single protein, with the four different mouse models arranged from left to right (p50 KO: green, miR/p50 DKO: yellow, WT: blue, miR KO: red). Each plot is composed of several thousand individual dots from several thousand single cells. The numbers on top represent the percentage of cytokine producing cells above the gate (the dotted line) and the bars represent the mean intensity of only the positive cytokine-producing cells (average intensity of the cells above the dotted line). C. A summary heat map showing the percentage of LSK cells that secrete any individual cytokine. D. Two-dimensional scatter plots showing protein-pair correlations. Results from p50 KO (green), WT (blue) and miR KO (red) LSK cells are plotted. Correlation coefficients (r value) of the two cytokines for the different mouse models are shown on the plots. E. A half-matrix summarizing the comparison of correlation coefficients (r values) of any given cytokine pairs between WT, p50 KO and miR KO LSK cells. Each square block, intercepted by two cytokines with one on the top and one to the right, represents correlation coefficients between the two cytokines. Green represents the case when WT LSK has the highest correlation, such as IL-6 vs. GM-CSF, and red represents when miR KO LSK has the highest correlation, such as IL-6 vs. IFN-γ. Correlations for all protein pairs from the p50 KO LSK cells are always lower than either WT or miR KO. F. Principal component analysis of LSK cells from the four genetic models. The data is plotted onto the two-dimensional space by the top two principal components. This reduced space is the one that can explain the most (>60%) information of the data. The directions of the two protein groups are represented by the two vectors aligned to the x-y axis.

NIH-PA Author Manuscript

NIH-PA Author Manuscript

NIH-PA Author Manuscript

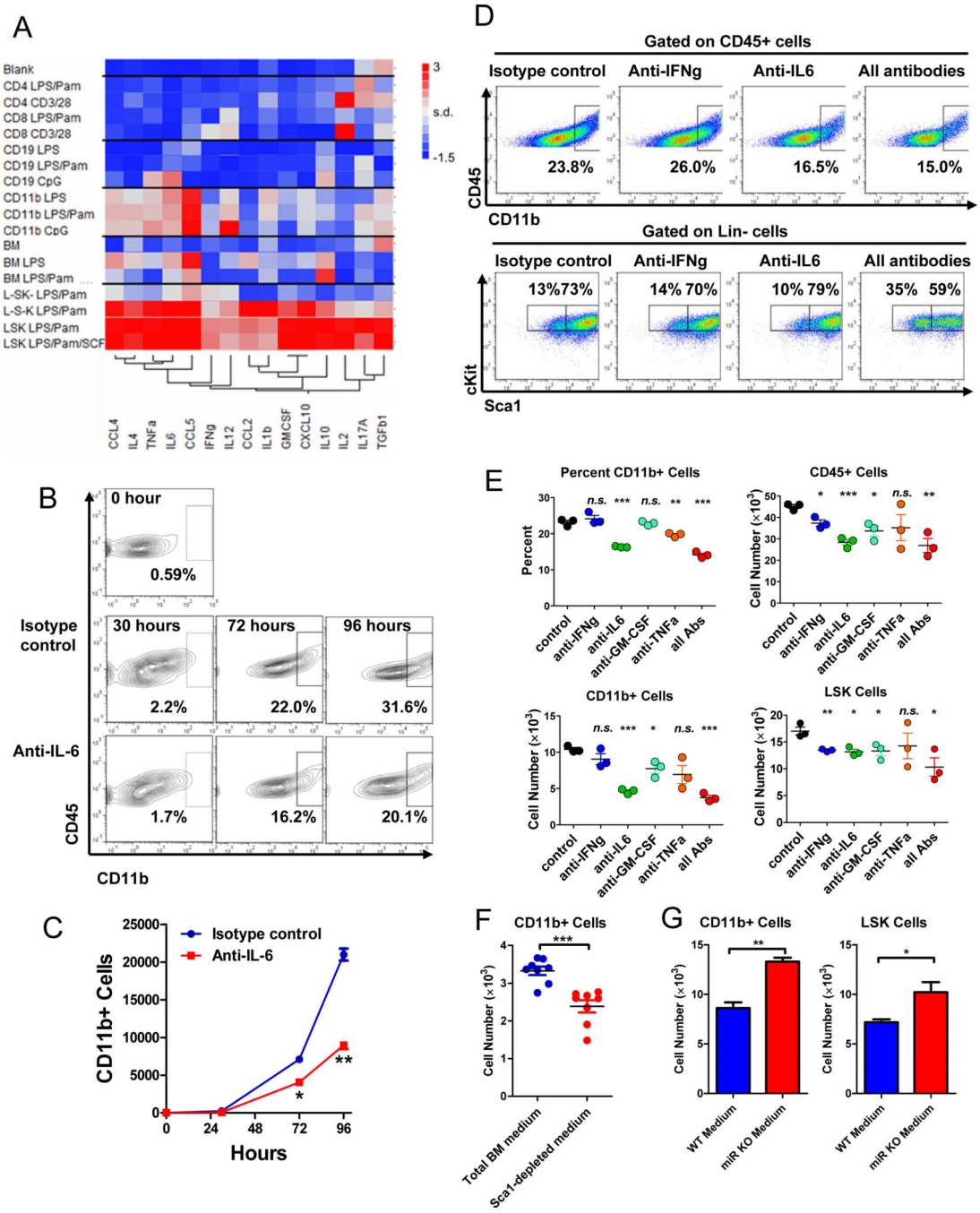

Figure 5. *In vitro* analysis of functional significance of HSPC-produced cytokines (see also Figure S5)

A. Multiplexed ELISA quantification of cytokines in bulk cell culture medium to compare cytokine production of different FACS purified cell subsets stimulated for 24 hours with various stimulations. Culture medium was collected and subjected to multiplexed ELISA quantification of 15 different cytokines and chemokines. Cell types include LSK cells, $L^-S^-K^+$ (Lineage$^-$Sca1$^-$cKit$^+$), and $L^-S^+K^-$ (Linage$^-$Sca1$^+$cKit$^-$) sorted from bone marrows and CD4$^+$ T cells, CD8$^+$ T cells, CD19$^+$ B cells, and CD11b$^+$ myeloid cells sorted from spleens. Stimulations include LPS/Pam (100ng/ml LPS and 1μg/ml Pam3CSK4),

NIH-PA Author Manuscript

NIH-PA Author Manuscript

NIH-PA Author Manuscript

LPS/Pam/SCF (100ng/ml LPS, 1μg/ml Pam3CSK4 and 50ng/ml stem cell factor), CpG (1μM), LPS (10ug/ml), CD3/28 (1μg/ml anti-CD3 and 1μg/ml anti-CD28). Blank, fresh medium; BM, culture medium from unstimulated total bone marrow cells. Data are presented as a heat map with low cytokine level represented in blue, intermediate level in white and high level in red. Cytokines are clustered into groups. B-E. Analysis of *in vitro* myelopoiesis from WT LSK cells by FACS. Sorted WT LSK cells were stimulated with LPS (100ng/ml), Pam3CSK4 (1μg/ml) and SCF (50ng/ml), in the presence of cytokine neutralizing antibodies. Control, isotype antibody control; all Abs, a combination of anti-IL-6, anti-IFN-γ, anti-GM-CSF and anti-TNF-α neutralizing antibodies. B and C. Timecourse of myelopoiesis from WT LSK cells in the presence of anti-IL-6 neutralizing antibody. D and E. Myelopoiesis from WT LSK cells in the presence of various neutralizing antibodies. Cells were analyzed on Day 3 by FACS for percent and number of myeloid cells and LSK cells. B and D are the representative FACS plots while C and E show the quantification (n=3). F and G. FACS analysis of *in vitro* myelopoiesis from WT LSK cells in the presence of conditioned medium. F. WT total bone marrow cells or WT bone marrow cells that have been depleted of $Sca1^{+}$ cells were stimulated with LPS and Pam3CSK4 for 24 hours to induce cytokine production into the culturing medium. The culturing medium from either total BM cells or sca1-depleted BM cells was then collected and used to stimulate freshly purified WT LSK cells. Number of myeloid and LSK cells was analyzed on Day 2 (n=8). G. WT or miR-146a KO LSK cells were stimulated with LPS and Pam3CSK4 for 24 hours to induce cytokine production into the culturing medium. The culturing medium from either WT or miR KO LSK cells was then collected and used to stimulate freshly purified WT LSK cells. Number of myeloid and LSK cells was analyzed on Day 2 (n=3). Data are presented as mean +/− s.e.m.

NIH-PA Author Manuscript

NIH-PA Author Manuscript

NIH-PA Author Manuscript

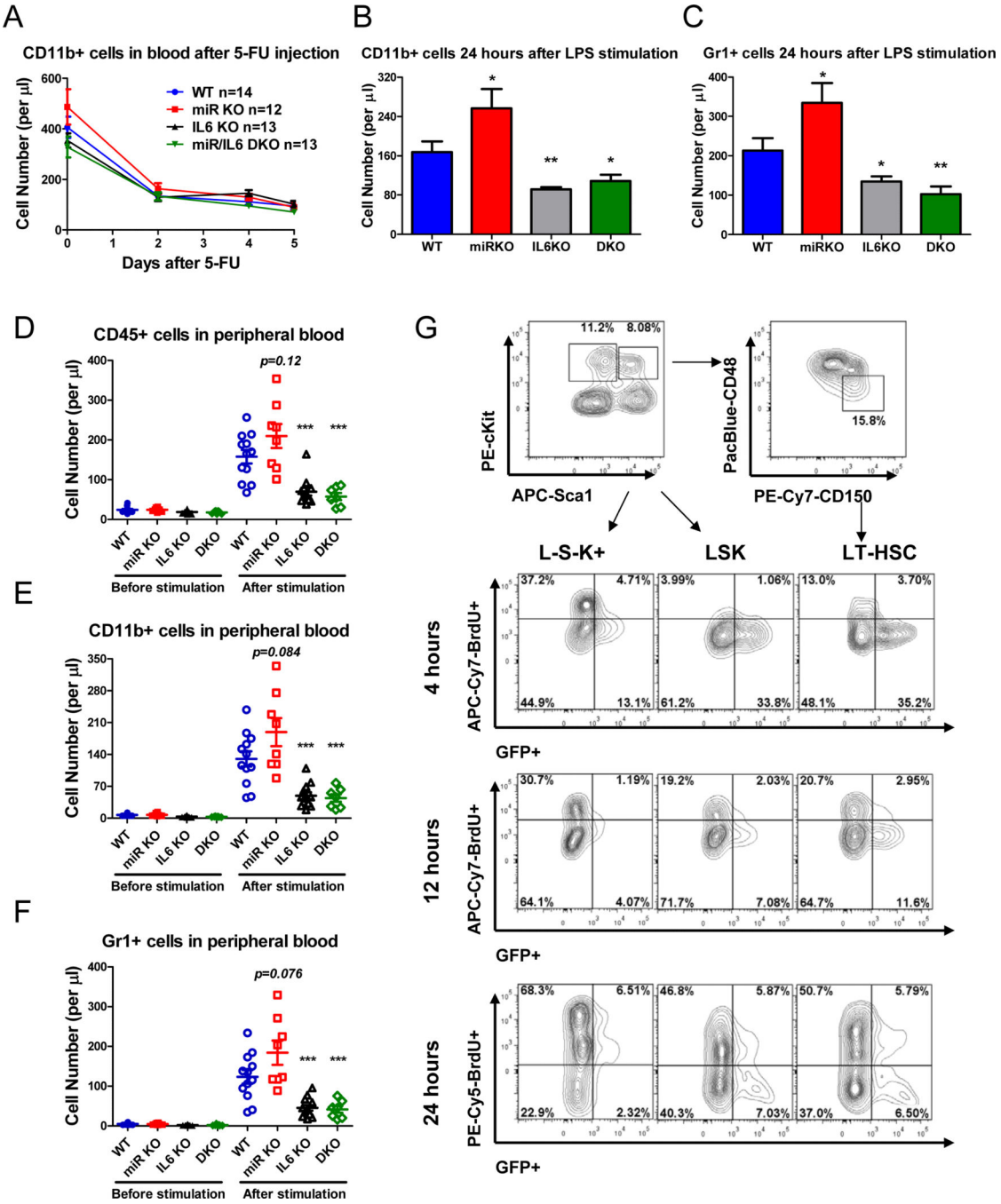

Figure 6. *In vivo* analysis of functional significance of HSPC-produced cytokines (see also Figure S6)

A-C. For 5-fluorouracil-induced neutropenia, WT, miR-146a KO, IL-6 KO and miR-146a/IL-6 DKO mice were injected with 5-fluorouracil (5-FU) (250 mg/kg of body weight, i.p.). A. Peripheral blood was analyzed on Day 0, 2, 4, and 5 by FACS to determine the number of $CD11b^+$ myeloid cells. On Day 5, LPS (0.3 mg/kg of body weight, i.p.) was injected and mice were bled 24 hours later to study LPS-induced myelopoiesis by analyzing the number of $CD11b^+$ (B) or $Gr1^+$ (C) cells. D-F. For stem cell transplant study, Lin^-cKit^+ cells were purified from the bone marrow of WT, miR-146a KO, IL-6 KO and miR-146a/IL-6 DKO

NIH-PA Author Manuscript

NIH-PA Author Manuscript

NIH-PA Author Manuscript

mice. 500,000 cells per mouse were injected intravenously into lethally irradiated WT recipient mice. On Day 6, mice were bled for FACS analysis to determine the degree of neutropenia. LPS was injected (0.3 mg/kg of body weight, i.p.) and 48 hours later, mice were bled to study LPS-induced myelopoiesis by analyzing the number of total white blood cells (D), $CD11b^+$ cells (E) and $Gr1^+$ cells (F). G. LPS (2 mg/kg of body weight, i.p.) and BrdU (1 mg, i.p.) were injected into NF-κBGFP transgenic reporter mice, which were harvested for FACS analysis at 4, 12 and 24 hours. Representative FACS plots of GFP expression and BrdU incorporation of $L^-S^-K^+$, LSK and HSCs. Data are presented as mean +/− s.e.m.